ELSEVIER

Journal of Alloys and Compounds 262–263 (1997) 169–174

Journal of ALLOYS AND COMPOUNDS

Angular dependence of metamagnetic transitions in RNi_2B_2C (R = Er, Ho, Dy, and Tb)

P.C. Canfield*, S.L. Bud'ko[1]

Ames Laboratory and Department of Physics and Astronomy, Iowa State University, Ames, IA 50011, USA

Abstract

The angular dependence of metamagnetic transitions is examined for RNi_2B_2C (R = Er − Tb) as a function of the angle the applied magnetic field makes with respect to the easy axis. For R = Ho and Dy the easy axis is [110] and for R = Er and Tb the easy axis is [100]. All four compounds manifest clear angular dependencies of three or more transitions. © 1997 Elsevier Science S.A.

Keywords: Angular dependence; Metamagnetic transitions; Applied magnetic field

1. Introduction

The superconducting and magnetic properties of the RNi_2B_2C (R = Gd − Lu) [1] have been studied in detail over the past 3 years. The interaction between local moment magnetism and superconductivity is clearly evident for R = *T*m − Dy, [2–5] while strong hybridization of the Yb *4f* levels with the conduction electrons leads to heavy fermion behavior in $YbNi_2B_2C$ [6,7]. In addition, the effects of non-locality have been seen to manifest themselves as a hexagonal to square vortex lattice transition in R = Y, Lu and Er compounds [8–10].

For R = Er − Tb there is an extreme magnetic anisotropy associated with the crystalline electric field (CEF) splitting of the Hund's rule ground state J-multiplet [3–5,11]. In each case the local moment is confined to the basal plane of the tetragonal unit cell for temperatures below roughly 100 K, i.e. temperatures well above the magnetic ordering temperatures. Recently, we have observed that there is a strong in-plane anisotropy, leading to the local moments essentially being confined to either the [100] (R = Er and Tb) or [110] (R = Ho and Dy) directions [12,13]. This in-plane anisotropy leads to a characteristic angular dependence of the metamagnetic transitions detected in the M(H) isotherms for H applied in the basal plane. In specific, for $HoNi_2B_2C$ there can be up to three metamagnetic transitions with angular dependencies of $H_{C1} = 4.1$ kG/cos(θ), $H_{C2} = 8.4$ kG/cos($\theta - 45$) and $H_{C3} = 6.6$ kG/sin($\theta - 45$), where θ is the angle that the applied magnetic field makes with respect to the easy axis while remaining perpendicular to the c-axis [12].

In this paper we report preliminary data and analysis of the anisotropic magnetization and the angular dependence of the metamagnetic transitions in R = Er, Dy, and Tb.

2. Experimental methods

All samples are single crystals of RNi_2B_2C that have been grown from Ni_2B flux [3]. The M(H,θ)

* Corresponding author.

[1] Present address: Dr. Xavier Sigaud 150, Rio de Janeiro, 22290-180, Brazil.

0925-8388/97/$17.00
PII S0925-8388(97)00374-5

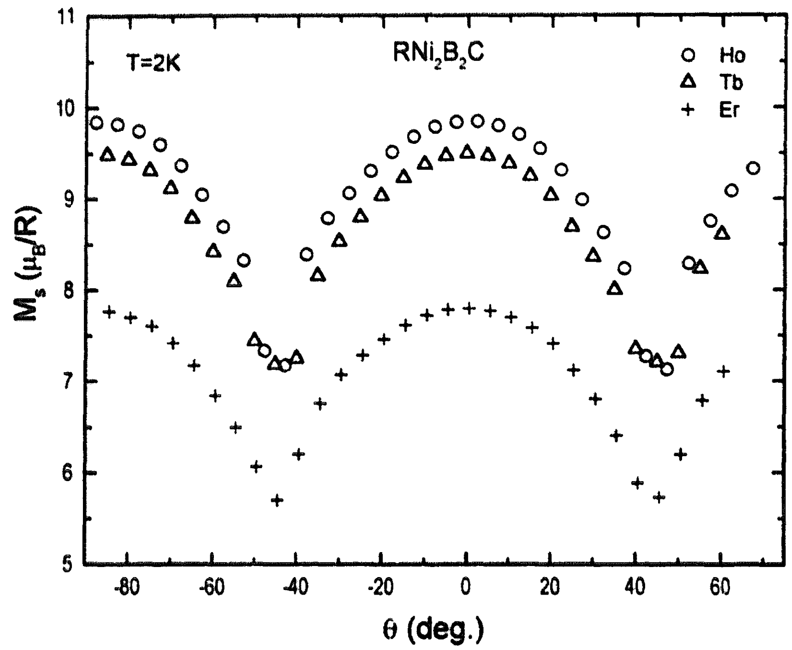

Fig. 1. Magnetization as a function of θ for $H = 55$ kG for RNi_2B_2C (R = Ho, Tb, Er).

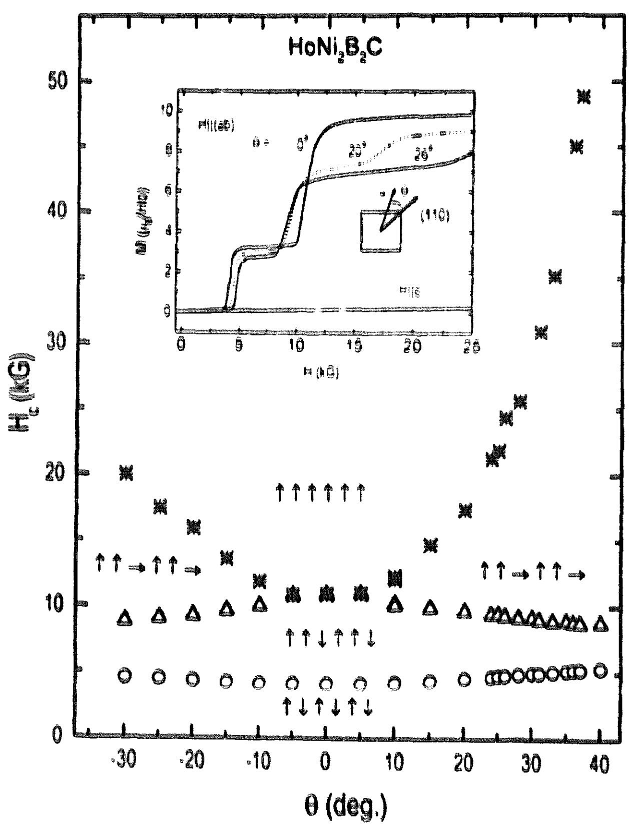

Fig. 2. Critical metamagnetic fields as a function of θ, $H_c(\theta)$, for $HoNi_2B_2C$ for $T = 2$ K. Inset: representative M(H) isotherms.

isotherms were taken using a modified Quantum Design rotator with the sample mounted in such a manner that H $\perp$ c-axis at all times. Magnetization data were taken either as a function of applied field with temperature and θ held constant, or as a function of θ with temperature and field held constant. All data were taken at $T = 2.0$ K.

3. Data and analysis

The four members of the RNi_2B_2C family studied (R = Er, Ho, Dy, and Tb) all have extreme planar anisotropy with each having an additional, distinct, in-plane anisotropy. Fig. 1 shows the high field (55 kG) longitudinal magnetization for $ErNi_2B_2C$, $HoNi_2B_2C$ and $TbNi_2B_2C$ as a function of θ. The easy axis for $ErNi_2B_2C$ and $TbNi_2B_2C$ is the [100] axis while the easy axis for $HoNi_2B_2C$ and $DyNi_2B_2C$ is the [110] axis. The angular dependence of all three data sets is well described by cos(θ) [12]. This is consistent with the local moments being fully along the easy axis and the measured longitudinal moment simply falling off as the projection of the local moment onto the applied field direction.

The angular dependencies of the metamagnetic transitions seen in $HoNi_2B_2C$ at 2 K are summarized [12] in Fig. 2. Depending upon the angle that the applied field makes with the [110] axis, up to three transitions can be seen. The two, lower field, transitions are bounded while the third transition diverges as $\theta \Rightarrow 45°$. The angular dependence of these three transition (see introduction) as well as the angular dependence of the locally saturated magnetization (between the transitions) can be explained via the assumption that the net distribution of moments along the four crystallographically similar [110] axes is ↑↓, ↑↑↓, ↑↑→ and ↑↑↑↑, where ↑ is a moment along the [110] axis, ↓ is a moment along the [$\bar{1}\bar{1}0$],

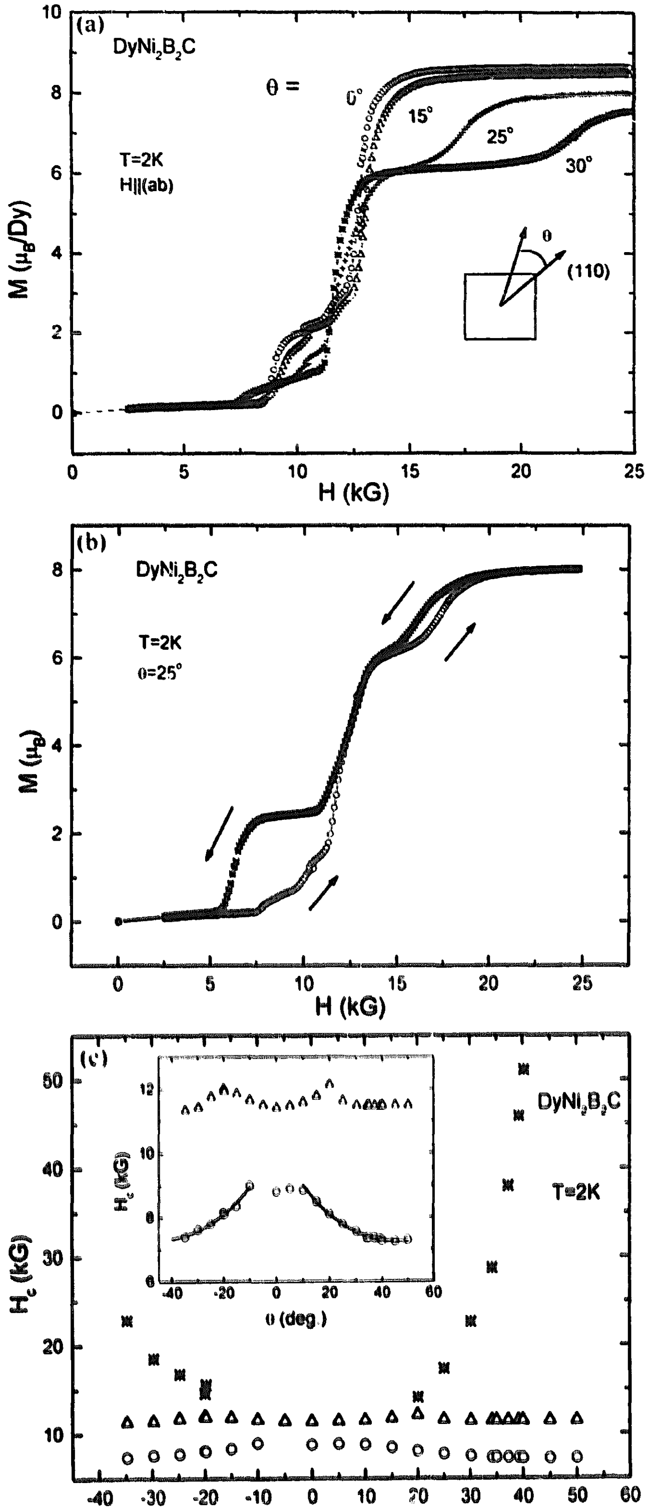

Fig. 3. (a) Representative M(H) isotherms for $DyNi_2B_2C$. (b) Applied magnetic field up/down hysteresis for representative M(H) isotherm. (c) $H_C(\theta)$ for $DyNi_2B_2C$ for $T = 2$ K. The solid line is 7.3 kG/cos($\theta - 45$).

and → is a moment along the [1$\bar{1}$0] axis [12]. For the lowest field region it is known that, at 2 K, the moments are in a commensurate antiferromagnetic state with ferromagnetically aligned basal planes that are rotated by 180° with respect to each other along the c axis [14,15]. The wave vector associated with the ↑↑↓ or ↑↑→ net distribution of moments is not known and ↑↑↑↑ is thought to be a saturated paramagnetic state.

In low fields, $DyNi_2B_2C$ orders in the simple commensurate antiferromagnetic structure that $HoNi_2B_2C$ adopts at low temperature [16]. In addition, $DyNi_2B_2C$ has the same easy axis [110], and a similar saturated moment [5]. With all these similarities, it is reasonable to assume that field-stabilized magnetic states in $DyNi_2B_2C$ will bear a strong similarity to those in $HoNi_2B_2C$. The data presented in Fig. 3a support this assumption. The primary difference between the $DyNi_2B_2C$ and $HoNi_2B_2C$ data is the relatively large, field up/field down, hysterisis found for $DyNi_2B_2C$ in the first metamagnetic transition (Fig. 3b). This hysterisis is much larger than that found in $HoNi_2B_2C$ (see [12] [Fig. 1b]). Fig. 3c shows the $H_C(\theta)$ phase diagram determined from Fig. 3a using only the onset of metamagnetism to give a single value for H_{C1}. In qualitative terms it is indeed similar to the phase diagram found for $HoNi_2B_2C$: two lower transitions that are bounded in field, and a third transition that is diverging as $\theta \Rightarrow 45°$. The significant quantitative differences are: (i) the larger angular range for which there is a transition directly from the first metamagnetic state to the saturated paramagnetic state (20° to −20°); and (ii) H_{C1} can not be cleanly fit to $1/\cos(\theta - 45)$ over the whole angular range due to the lack of cusps for $\theta \Rightarrow 0°$. This latter difference may be due to our method of determining H_{C1} in the highly hysteretic, low field region.

$ErNi_2B_2C$ is another superconducting member of the series, but the easy axis of $ErNi_2B_2C$ is along the [100] direction and the low temperature, low field, magnetically ordered state has a wave vector of $q = 0.55\ a^*$ [17,18]. Fig. 4a presents a manifold of M(H) isotherms. As θ is increased the lower two transitions move up in field, the third transition is relatively insensitive to θ and there is a subtle, final transition with a critical field that diverges as $\theta \Rightarrow 45°$. The angular dependencies of these critical fields are shown in Fig. 4b. The lower two critical fields (inset) are well fitted by 7.4 kG/cosθ and 11.1 kG/cosθ. The field up/field down hysterisis for $ErNi_2B_2C$ is relatively small, being comparable to that seen for $HoNi_2B_2C$.

$TbNi_2B_2C$ does not superconduct for temperatures above 0.3 K [19] and has [100] as the easy axis. Like $ErNi_2B_2C$, $TbNi_2B_2C$ orders in low fields with a $q \sim 0.55\ a^*$ wave vector. Fig. 5a presents a manifold of M(H) isotherms and Fig. 5b is the $H_C(\theta)$ phase diagram. The first metamagnetic transition, H_{C1}, follows 12.1 kG/cosθ angular dependence (solid line), and, like $ErNi_2B_2C$ there is a weak high field transi-

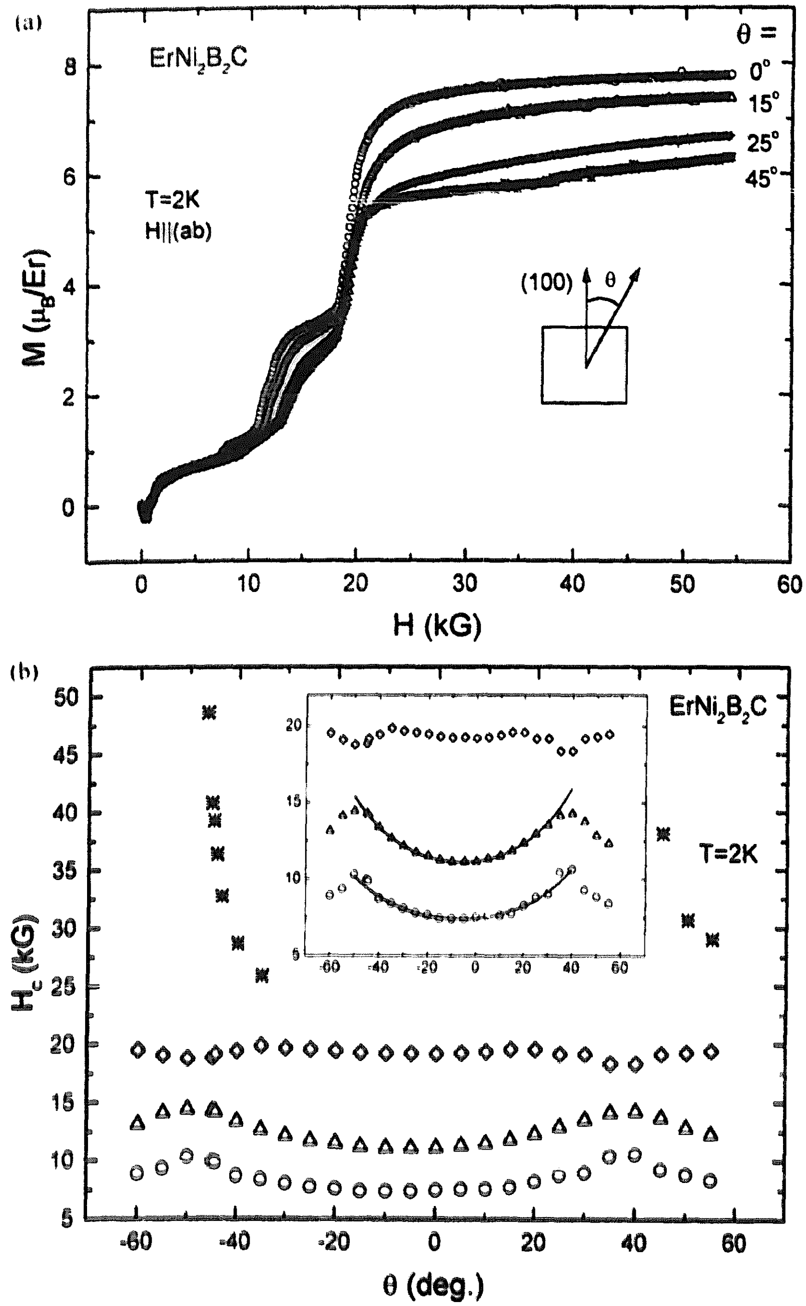

Fig. 4. (a) Representative M(H) isotherms for $ErNi_2B_2C$. (b) $H_c(\theta)$ for $ErNi_2B_2C$ for $T = 2$ K (Solid lines in inset are 7.4 kG/cosθ and 11.1 kG/cosθ.

tion that diverges as $\theta \Rightarrow 45°$. Instead of a clear, well defined H_{c2}, there appear to be up to three, closely spaced transitions for 20 kG < H < 30 kG.

Some basic trends can be seen to emerge from these data. $HoNi_2B_2C$ and $DyNi_2B_2C$ both have the [110] as the easy axis. They both order in a commensurate antiferromagnetic ground state at 2 K in low field, and in both cases the final transition is clearly resolvable and diverges as $\theta \Rightarrow 45°$. $ErNi_2B_2C$ and $TbNi_2B_2C$ both have [100] as the easy in axis. Both of these compounds have magnetic ordering with $q \approx 0.55\ a^*$ and at 2 K both have a ferrimagnetic component associated with the low field magnetization [11,13]. Both of these compounds have a faint upper transition that diverges as $\theta \Rightarrow 45°$. In addition, while all compounds have some field up/field down hysterisis, $DyNi_2B_2C$ has a large hysterisis associated with the low field metamagnetic transitions.

Acknowledgements

We would like to thank Alex Panchula for his help in figure preparation. Ames Laboratory is operated for the US Department of Energy by Iowa State

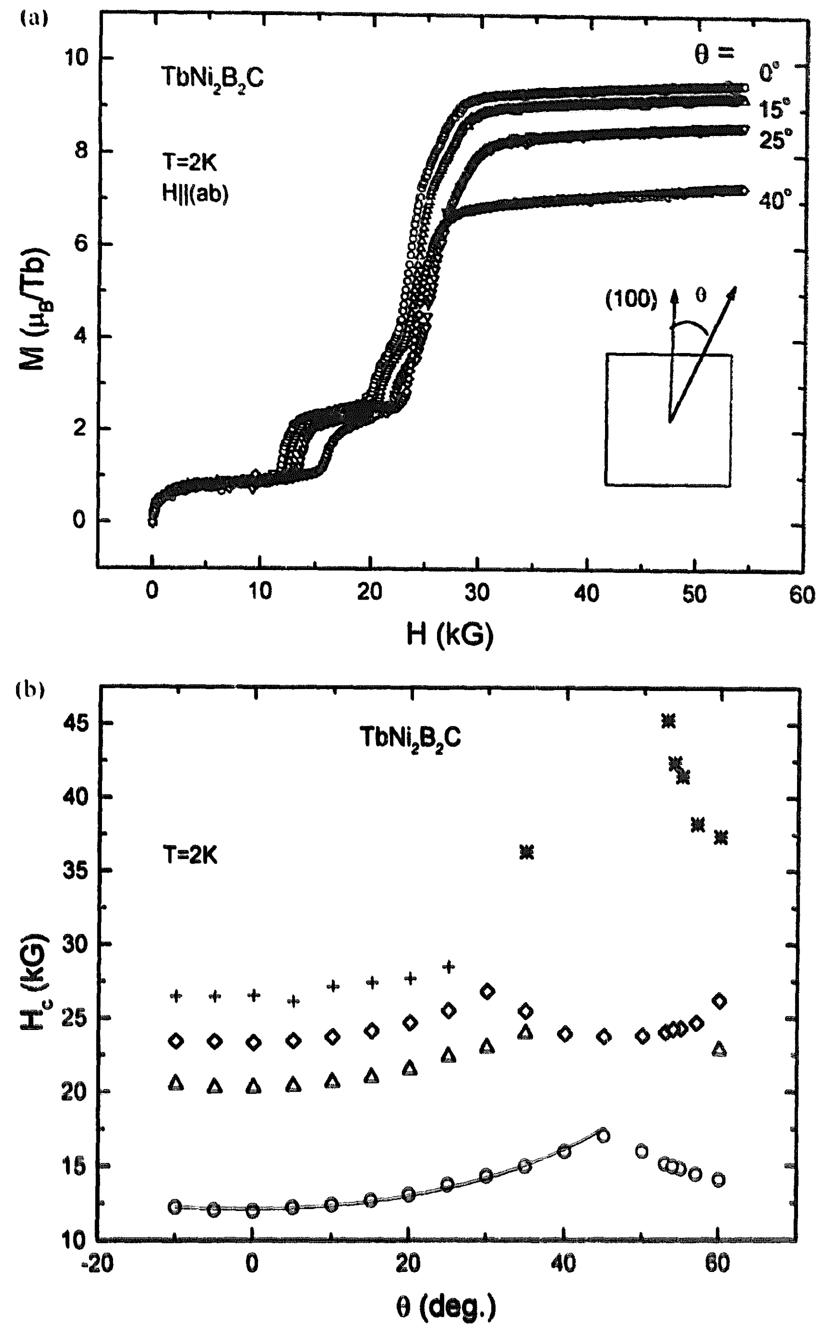

Fig. 5. (a) Representative M(H) isotherms for $TbNi_2B_2C$. (b) $H_C(\theta)$ for $TbNi_2B_2C$ for $T = 2$ K. The solid line is 12.1 kG/cosθ.

University under Contract Number W-7405-Eng-82. This Work was supported by the Director for Energy Research, Office of Basic Energy Science.

References

[1] R.J. Cava, et al., Nature 367 (1994) 252.

[2] B.K. Cho, M. Xu, P.C. Canfield, L.L. Miller, D.C. Johnston, Phys. Rev. B 52 (1995) 3676.

[3] B.K. Cho, P.C. Canfield, L.L. Miller, D.C. Johnston, W.P. Beyermann, A. Yatskar, Phys. Rev. B 52 (1995) 3684.

[4] K.D.D. Rathnayaka, D.G. Naugle, B.K. Cho, P.C. Canfield, Phys. Rev. B 53 (1996) 5688.

[5] B.K. Cho, P.C. Canfield, D.C. Johnston, Phys. Rev. B 52 (1995) R3844.

[6] A. Yatskar, N.K. Budraa, W.P. Beyermann, P.C. Canfield, S.L. Bud'ko, Phys. Rev. B 54 (1996) R3772.

[7] S.K. Dhar, et al., S.S. Comm. 98 (1996) 985.

[8] M.R. Eskildsen, P.L. Gammel, B.P. Barber, A.P. Ramirez, D.J. Bishop, N.H. Anderson, K. Mortensen, C. Bolle, C.M. Lieber, P.C. Canfield, Phys. Rev. Lett. (in press).

[9] U. Yaron, P.L. Gammel, A.P. Ramirez, et al., Nature 382 (1996) 236.

[10] M.R. Eskildsen, P.L. Gammel, B.P. Barber, U. Yaron, et al., Phys. Rev. Lett. 78 (1997) 1968.

[11] B.K. Cho, P.C. Canfield, D.C. Johnston, Phys. Rev. B 53 (1996) 8499.

[12] P.C. Canfield, S.L. Bud'ko, B.K. Cho, et al., Phys. Rev. B 55 (1997) 970.
[13] P.C. Canfield, S.L. Bud'ko, B.K. Cho, Physica C 262 (1996) 249.
[14] A.I. Goldman, C. Stassis, P.C. Canfield, et al., Phys. Rev. B 50 (1994) R9668.
[15] T.E. Grigereit, et al., Phys. Rev. Lett. 73 (1994) 2756.
[16] P. Dervenagas, J. Zarestky, C. Stassis, A.I. Goldman, P.C. Canfield, B.K. Cho, et al., Physica B 212 (1995) 1.
[17] J. Zarestky, C. Stassis, A.I. Goldman, et al., Phys. Rev. B. 51 (1995) R678.
[18] S.K. Sinha, et al., Phys. Rev. B 51 (1995) R681.
[19] C.V. Tomy, et al., Phys. Rev. B 53 (1996) 307.